HHS Public Access

Author manuscript

Dev Dyn. Author manuscript; available in PMC 2018 August 01.

Published in final edited form as:

Dev Dyn. 2017 August ; 246(8): 625–634. doi:10.1002/dvdy.24524.

A Role for Primary Cilia in Aortic Valve Development and Disease

Katelynn A Toomer[1], **Diana Fulmer**[1], **Lilong Guo**[1], **Alex Drohan**[1], **Neal Peterson**[1], **Paige Swanson**[1], **Brittany Brooks**[1], **Rupak Mukherjee**[2,3], **Simon Body**[4], **Josh Lipschutz**[3,5], **Andy Wessels**[1], and **Russell A. Norris**[1,5,*]

[1]Department of Regenerative Medicine and Cell Biology, Medical University of South Carolina, Charleston, SC, 29425 USA

[2]Division of Cardiothoracic Surgery, Department of Surgery, Medical University of South Carolina, Charleston, SC, 29425

[3]Department of Medicine, Ralph H. Johnson Veterans Affairs Medical Center, Charleston, SC, 29425 USA

[4]Department of Anesthesiology, Perioperative and Pain Medicine, Brigham and Women's Hospital, Harvard Medical School, Boston, Massachusetts, 02115, USA

[5]Department of Medicine, Medical University of South Carolina, Charleston, SC, 29425 USA

Abstract

Background—Bicuspid aortic valve (BAV) disease is the most common congenital heart defect affecting 0.5–1.2% of the population and causes significant morbidity and mortality. Only a few genes have been identified in pedigrees and no single gene-model explains BAV inheritance, thus supporting a complex genetic network of interacting genes. However, patients with rare syndromic diseases that stem from alterations in the structure and function of primary cilia ("ciliopathies") exhibit BAV as a frequent cardiovascular finding, suggesting primary cilia may factor broadly in disease etiology.

Results—Our data are the first to demonstrate that primary cilia are expressed on aortic valve mesenchymal cells during embryonic development and are lost as these cells differentiate into collagen-secreting fibroblastic-like cells. The function of primary cilia was tested by genetically ablating the critical ciliogenic gene, *Ift88*. Loss of *Ift88* resulted in abrogation of primary cilia and increased fibrogenic ECM production. Consequentially, stratification of ECM boundaries normally present in the aortic valve were lost and a highly penetrant BAV phenotype was evident at birth.

Conclusions—Our data support cilia as a novel cellular mechanism for restraining ECM production during aortic valve development and broadly implicate these structures in the etiology of BAV disease in humans.

Correspondence: Russell A. Norris, PhD. Cardiovascular Developmental Biology Center, Department of Regenerative Medicine and Cell Biology, 171 Ashley Avenue, Charleston, SC, 29425, Office: 608 Children's Research Institute, Lab: 604F Children's Research Institute, Phone: (843) 792-3544 (office), Phone: (843) 792-1544 (lab), Fax: (843) 792-0664, norrisra@musc.edu.

Keywords

Primary Cilia; Bicuspid Aortic Valve; Cardiac Development; Extracellular Matrix

Introduction

Bicuspid aortic valve (BAV) disease is the most common congenital valvular heart defect affecting 0.5–1.2% of the population and is a significant cause of morbidity and mortality. Comorbidity of other cardiovascular disease often segregate with BAV, including ascending aortic dilation, aortic stenosis (AS), coarctation of the aorta, and calcific aortic valve disease (CAVD) occurring 10–20 years prior to population norms (Tzemos et al., 2008; Michelena et al., 2011; Martin et al., 2015). There is no curative or preventative medical therapy for these aortic diseases and, in North America alone, 80,000 patients progress annually to severe symptomatic CAVD requiring aortic valve replacement (AVR). The lack of therapies may be attributed to a paucity of genetic and biological data underlying the clinical aspects of this disease. To date, only a few genes have been identified in pedigrees and it is clear that no single gene-model explains BAV inheritance, thus supporting a complex genetic network of interacting genes (Garg et al., 2005; Bonachea et al., 2014a). Nonetheless, the high prevalence of BAV and its anatomically discrete, but frequent, co-existing diseases, support a potential unifying molecular genetic cause of the disease. This contention is further supported by clinical findings in patients with complex congenital diseases associated with disruption of primary cilia known as “ciliopathies”. Patients with ciliopathic diseases commonly present with cardiac defects that include bicuspid aortic valve disease and/or aortic stenosis (Karp et al., 2012). These clinical findings motivated our studies to examine the potential role of primary cilia in aortic valve development and disease.

Cilia are microtubule-containing structures (axonemes) that project from the cell. There are two main types of cilia: motile and immotile. Motile cilia (100’s/cell) are primarily involved in fluid movements. In contrast, immotile cilia (a.k.a. primary cilia) are solitary (1/cell), extend from the anchoring basal body and function as cellular “antennae” to coordinate various signaling pathways (Ishikawa and Marshall, 2011) such as Notch1 (Liu et al., 2007; Samsa et al., 2015; Grisanti et al., 2016; Li et al., 2016), Hedgehog (Echelard et al., 1993), Wnt (Lienkamp et al., 2012), PDGF (Schneider et al., 2005; Clement et al., 2013b), and TGFβ (Clement et al., 2013a) as well as function as calcium sinks (Delling et al., 2013) and potentially as mechanosensors on endothelial cells (Jin et al., 2014). Although primary cilia have been previously linked to congenital heart malformations, such as heterotaxy and atrioventricular septal defects (Li et al., 2004; Hoffmann et al., 2009; Friedland-Little et al., 2011; Hoffmann et al., 2014; Li et al., 2015), the role of these structures in the aortic valves is unknown.

In this study, we uncover three novel aspects of primary cilia during development. First, primary cilia are expressed predominantly on aortic valve interstitial cells in a spatio-temporal manner, while being scantly observed on valve endocardium. Second, genetic ablation of primary cilia results in highly penetrant myxomatous bicuspid aortic valve disease, similar to the cardiac phenotype observed in ciliopathy patients. Third, we show that

primary cilia restrain extracellular matrix expression, suggesting cilia play a role in suppressing differentiation of aortic valve mesenchymal cells in a temporal manner. Thus, these studies are the first to identify a morphogenetic link between primary cilia and aortic valve disease and support a model whereby primary cilia are not only cellular antennae, but also cellular clocks that dictate the temporal activation of differentiation. Additionally, due to the indispensable role for cilia in regulating various growth factor signaling pathways, these structures may play a broad role in bicuspid aortic valve disease in humans.

Results and Discussion

Temporal-Spatial Analyses of Primary Cilia During Aortic Valve Development

By combining specific primary cilia markers with high-resolution confocal microscopy, we were able to gain a quantitative map of primary cilia during valvulogenesis. We initially focused on the presence and length of primary cilia (Figure 1). We focus on cilia length due to the recognition that length is a major predictor of proper cilia function. Inappropriate elongation of primary cilia can hinder the biological processes in which cilia function and several ciliopathies have been associated with defects in cilia length (Niggemann et al., 1992; Yuan et al., 2012; Broekhuis et al., 2013; Broekhuis et al., 2014). Our data demonstrate that primary cilia are present on interstitial cells of the developing outflow tract cushions at E11.5 and E13.5, while being rarely observed on the valve endocardium (Figure 1A). As development proceeds into fetal life, these structures grow in length, reaching a maximum average length of 2.5–3.0 μm by E17.5. During postnatal growth of the heart, primary cilia become shorter and are gradually lost with adult aortic valve interstitial cells (aVICs) rarely expressing these structures (Figure 1A, B).

Additional expression studies also identified primary cilia as not only being temporally regulated but that they also become restricted to specific ECM zones within the aortic valves (Figure 2). For example, primary cilia are observed at early timepoints of valve development when the primitive cuspal tissue is comprised mostly of mesenchymal cells bathed in a provisional ECM that includes abundant proteoglycans (e.g. versican and hyaluronan) (Figure 2A). Subsequently, during fetal and early postnatal aortic cusp maturation, mesenchymal cells transition (or differentiate) into a fibroblast-like phenotype and increase expression and deposition of various collagens (e.g. collagen type I) (de Vlaming et al., 2012). During this transitional timepoint, primary cilia within the collagen-rich fibrosa layer of the aortic cusps are drastically reduced in both numbers and length (Figure 2B,C). This would suggest that either the interstitial cells are no longer responding to pro-ciliogenic factors and/or that the changing ECM environment negatively feeds back to suppress ciliogenesis. Consistent with this latter notion, prior work in other tissues have supported a role for the ECM in regulating cilia function (Christensen et al., 2008; Seeger-Nukpezah and Golemis, 2012). This is particularly evident in vascular smooth muscle cells whereby cilia, and ultimately differentiation, is regulated in part by the metalloproteinase, ADAMTS9 (Nandadasa et al., 2015).

The timing in which we observe cilia disappear from specific zones within the aortic valves also coincides with increasing biomechanical stresses. Blood volume and pressure increases, which likely trigger mechanosensitive stimuli on aortic valve interstitial cells. Interestingly,

previous reports suggested that primary cilia are expressed by endocardial cells of the early valve primordia in areas of low-shear stress, thus supporting a mechanosensing role (Egorova et al., 2011). While the primary cilia in the aortic valve may indeed have a mechanosensing role, it is unlikely that cilia on the endocardial surface would serve this function due to their short length and sparse presence on the valve endocardium (Figure 1 and 2). This, however does not preclude the role of mechanosensing of cilia in the valve interstitium. Indeed, compression (from clasping of cuspal tissue together), tension (albeit limited in the aortic cusps), and interstitial flow (which occurs in proteoglycan-rich, water loving environments where cilia are concentrated—Figure 2B, C) are biomechanical stimuli that valve interstitial cells sense on a beat-by-beat basis during the cardiac cycle. Thus, we cannot rule out a mechanosensing role for primary cilia in the proteoglycan-rich spongiosa regions in which they are retained during fetal and early postnatal life.

Active Hedgehog signaling during aortic valve development—In addition to potential mechanical stresses, it is clear that cilia respond to growth factor signals (hedgehog, Tgfβ, Notch, Wnt, Pdgf). Since the hedgehog pathway had previously not been investigated in the aortic valves, 3D-immunohistochemistry (3D-IHC) was performed for major constituents of this signaling pathway. As shown in Figure 3, 3D-IHC confirmed that smoothened (a G-protein coupled receptor that interacts with the hedgehog receptor, Patched) and Gli3 (a key transcription factor that transmits hedgehog signals) are expressed by aVICs. Interestingly, our studies also show smoothened protein (arrowheads in Figure 3A) in transit along the cilia axoneme (green staining in Figure 3A). Movement of smoothened into the axoneme is not only a required regulatory step in promoting Gli3 activation but also signifies active hedgehog signaling in the aortic valves. Currently, which of the three-known hedgehog ligand(s) (sonic, indian, or desert) are responsible for activating this pathway is unknown. Previous in situ data has demonstrated that sonic and indian hedgehog are not expressed in the valve primordia making them unlikely candidates. Desert hedgehog, however, appears to be robustly expressed in the developing cushion endocardium (Bitgood and McMahon, 1995), suggesting a putative cross-talk mechanism between desert secreting endocardial cells and respondent cilia-containing aVICs.

Primary cilia and bicuspid aortic valves—To test the function of primary cilia, we genetically ablated the axoneme during aortic valve development by conditionally removing the *Ift88* gene. Ift88 is an intraflagellar transport protein that acts as a scaffold for vesicular transport up and down the ciliary axoneme and has been shown to be essential for the formation and maintenance of primary cilia (Pazour et al., 2000). Loss of *Ift88* results in either total deletion or very short ciliary axonemes and early embryonic lethality (Pazour et al., 2000; Sun et al., 2004; Veland et al., 2009). To circumvent embryonic lethality and test the function of primary cilia in the aortic valve, we employed a conditional approach whereby the floxed Ift88 allele ($Ift88^{f/f}$) was bred to a cardiac endocardial-specific Cre driver, ($NfatC1^{Cre(+)}$) known to be active during aortic valve morphogenesis (Zhou et al., 2002; Wu et al., 2012). As shown in Figure 4A, conditional loss of *Ift88*, results in profound shortening and/or complete loss of axonemes in the aortic leaflets. Due to the contributions of multiple cell-lineages (i.e. neural crest, second heart field, endocardium) to the developing aortic valves, not every aVIC has lost its primary cilia. Nonetheless, endocardial-

derived cells (in which the *NfatC1*^{Cre} is active) represent a major contributing cell source to the aortic cusps and histological analyses of *Ift88* deficiency (*NfatC1*$^{Cre(+)}$; *Ift88*$^{f/f}$) in this cell type revealed an enlargement of the hinge regions between the right and non-coronary leaflets, indicative of a bicuspid aortic valve phenotype (Figure 4B). Three-dimensional reconstructions demonstrated the presence of two instead of three cusps in the conditional knockout when compared to littermate controls. This phenotype was highly penetrant, being observed in 19 out of 28 (68%) total conditional knockout animals analyzed.

Primary cilia and differentiation vs. proliferation—To elucidate the mechanism(s) by which this BAV phenotype occurs, we assayed whether cilia deficient aortic valves result in altered proliferation and/or extracellular matrix production. Contrary to prior studies on primary cilia, loss of axonemes in the aortic valves failed to reveal statistically significant changes in cell proliferation as assayed by Ki67 and pHH3 (Figure 5A, B), total cell number (Figure 5B), or apoptosis (data not shown). Since there are no changes in total cell number or proliferation/apoptosis, this would seemingly exclude a role for primary cilia in regulation of EMT, as previously described (Egorova et al., 2011). Next, we investigated whether increased ECM may provide an explanation for increased cuspal size. Cell density and immunohistochemical stains confirmed a significant decrease in cell density (Figure 5C, D) and an increase in the production of ECM substrates (e.g. collagen I and versican) (Figure 5E–G). These data support the contention that primary cilia restrain valve size and can either directly or indirectly alter production of critical ECM components, versican and collagen I. This observation is consistent with previous reports of cilia function in various tissues and species. For example, studies in zebrafish and mice have shown that primary cilia regulate ECM composition through transcriptional control of small leucine rich proteoglycans (SLRPs) (Huang et al., 2013), metalloproteinases (e.g. Adamts5) (Thompson et al., 2014) or collagen genes (Mangos et al., 2010) in kidney and bone. Interestingly, an ECM feedback loop is also involved in ciliary signaling and the ECM itself can affect ciliary structure and function as is evident with loss of function of Adamts9 (Nandadasa et al., 2015). In each of these cases, loss of primary cilia or alteration of the ECM milieu results in pathological tissues. Additionally, loss of function models in ADAMTS genes (targets of cilia signaling) have been shown to result in congenital BAV in various mouse models (Dupuis et al., 2013). These data demonstrate that primary cilia are not simply vestigial organelles leftover from evolution, but rather dynamic cellular appendages that regulate critical morphogenetic process required for normal aortic valve development.

Ciliopathies and aortic valve disease—Human genetic and clinical data have demonstrated that patients with defects in primary cilia (“ciliopathies) have increased incidence of aortic valve defects (Karp et al., 2012). Many adult aortic diseases, especially bicuspid aortic valve disease, have a congenital etiology and progress to clinically relevant disease in the adult that can be characterized by calcification, stenosis, and/or aortic insufficiency. A hallmark of these diseased valves is a myxomatous phenotype with increased proteoglycans and fragmented collagen (Hinton et al., 2008; Martin et al., 2015; Mathieu et al., 2015). Additionally, pediatric BAV disease cases are defined, at least in part, by excessive and disorganized ECM production with no change in proliferation (Hinton et al., 2006). Thus, we evaluated whether adult aortic valves from conditional knockout mice

(*Nfatc1*$^{(Cre+)}$;*Ift88*$^{f/f}$) vs control littermates exhibit increased expression of collagen and versican. As shown in Figure 6, the consequence of developmental loss of primary cilia on endocardial-derived cells is increased collagen and versican, which are no longer restricted to the fibrosa and spongiosa, respectively. Rather, their pattern of expression is broadened and overlapping, resulting in blurring of zonal molecular boundaries in the aortic cusps, signifying a myxomatous phenotype. Quantification of cell density also showed decreased cell density (Figure 6B, C), consistent with our developmental studies. Interestingly, Herovici stains, which mark mature collagen fibers in red (Levame and Meyer, 1987; Rawlins et al., 2006) were easily discernible in the wildtype aortic valves and correlated well with the collagen localization in the fibrosa layer of the aortic valve through IHC and histological techniques (Movat's Pentachrome) (Figure 6A, D—black arrowheads). On the contrary, whereas cilia deficient adult aortic cusps exhibit increased collagen expression by IHC compared to controls, they failed to show Herovici-positive red stain in the aortic cusps (Figure 6D—black arrows). Thus, the lack of cilia not only increases collagen synthesis but likely renders the cells incapable of processing this collagen into mature fibers.

Due to the clinical correlation between bicuspid aortic valve disease and calcific aortic stenosis, aberrant chondrogenic and/or calcific differentiation of the aVICs was evaluated in cilia deficient aortic cusps. Although we did observe a preponderance of chondrocytes at the aortic hinge region (Figure 6—red arrow), alizarin red and Von Kossa stains did not reveal consistent evidence of calcification (data not shown). Due to the age of the mice evaluated (4 months), future studies will focus on the possibility for calcification in older (>1 year) cilia-deficient animals, as is observed in the aged human population.

Concluding Perspectives—Although the presence and function of primary cilia is becoming better understood in various cell types, their role in cardiac development is still in its infancy. Herein we report the first documentation of primary cilia in the developing aortic valves and show that perturbation of these structures results in aortic valve defects. We demonstrate that primary cilia function to restrain ECM production, supporting a role for these structures in the temporal activation of a differentiation program. Premature accumulation of fibrogenic ECM and decreased cell density contributed to the increased size of the aortic cusps and correlated with a highly penetrant BAV phenotype observed in cilia deficient animals. Although this report details the presence and function of primary cilia in the aortic valves, future concerted efforts will be needed to identify whether primary cilia are broadly applicable to other sets of valves. On this note, clinical findings in patients with ciliopathies support a key role for primary cilia in the mitral, tricuspid and pulmonary valves. For example, patients with autosomal dominant polycystic kidney disease (ADPKD) have a 10-fold increase incidence of mitral valve prolapse (Lumiaho et al., 2001), while patients with Ellis-van Creveld (EVC) syndrome (Baujat and Le Merrer, 2007) and Nephronophthisis (NPH) commonly display mitral insufficiency (Tory et al., 2009). Tricuspid and pulmonary valve defects and/or stenosis are also found in patients with Bardet-Biedl syndrome (Elbedour et al., 1994; Cherian and Al-Sanna'a, 2009; Deveault et al., 2011), EVC (Baujat and Le Merrer, 2007), and NPH (Tory et al., 2009). Thus, cilia in the other sets of valves may play critical, and as yet unexplored roles in the etiology and progression of clinically-relevant valve diseases.

To date, only a few genes have been identified in pedigrees, and it is clear that no single gene-model explains BAV inheritance, thus supporting a complex genetic network of interacting genes. Nonetheless, the high prevalence of BAV and its anatomically discrete, but frequent, co-existing diseases, support a potential unifying molecular genetic cause of the disease. Support for this unification concept comes from previous reports that demonstrate primary cilia are required for regulating the function of Notch1 (Grisanti et al., 2016), PDGF (Schneider et al., 2005; Clement et al., 2013b), Tgfβ (Clement et al., 2013a), Wnt signaling (Lienkamp et al., 2012; Bonachea et al., 2014b), and Gata transcription factors (Daoud et al., 2014), genes and pathways that have been associated with BAV phenotypes (Garg et al., 2005; Bonachea et al., 2014a; Bonachea et al., 2014b; Daoud et al., 2014). Additional clinical support for primary cilia in aortic valve diseases stems from phenotypic data obtained from patients with ciliopathies, syndromic diseases that stem from disrupted cilia structure and/or function. For example, patients with Joubert (Karp et al., 2012), Bardet-Biedl (Elbedour et al., 1994; Deveault et al., 2011), Cranioectodermal dysplasia (CED) (Levin et al., 1977) or Meckel-Gruber (Salonen, 1984) syndromes have been reported with bicuspid aortic valves and/or aortic stenosis. Thus, the genetic mechanisms underlying the formation of cilia (aka ciliogenesis) and propagation of ciliogenic signals may, in the future, support disrupted cilia as a frequent cause of BAV. Completion of additional genetic screens in patients with BAV will undoubtedly shed light on this potential, and may provide a common drugable ciliogenic pathway that could be used for patient benefit.

Experimental Procedures

Mouse Studies

Ift88 conditional mice and genotyping were a kind gift from Dr. Courtney Haycraft and described previously(Haycraft et al., 2007). Histology was performed on embryonic and adult wild-type (*NfatC1*$^{Cre-}$;*Ift88*$^{f/f}$) and conditional knockout (*NfatC1*$^{Cre+}$;*Ift88*$^{f/f}$) hearts on mixed background. All mouse experiments were performed under protocols approved by the Institutional Animal Care and Use Committee, Medical University of South Carolina. Prior to cardiac resection, mice were euthanized in accordance with the Guide for the Care and Use of Laboratory Animals (NIH Publication No. 85-23, revised 1996.)

Each of the experimental paradigms established in this proposal were performed blinded to genotype and evaluated by multiple investigators to assure data interpretation was not biased. In each of the experiments, sample sizes were chosen to provide power of 0.8 to detect biological significant differences between test groups with two-sided $\alpha = 0.05$. Assumptions of normal distributions were made for quantitative biological measurements and comparison groups were assumed to have similar variances. Great care was taken to consider potential differences in phenotypes between male and female animals. Thus, female and male samples were analyzed separately for genotypic and phenotypic variations. Our outcomes failed to identify statistical differences between gender in each of the studies, thereby justifying pooling of phenotypic data. Data is displayed as combined male and female

Histology, Immunohistochemistry/Immunofluorescence

Embryonic and adult tissue were processed for hematoxylin and eosin (H and E) staining, Herovici's collagen stain and, immunohistochemistry/immunofluorescence (IHC) as previously described (Dina et al., 2015; Durst et al., 2015; Sauls et al., 2015). IHC of cilia stains to look at expression and measure cilia length were done on 15 μm thick sections to insure measurement of full cilia length. Histology and IHC were preformed using 5 μm thick sections from E11,13,15,17, P0, and Adult (4month) aortic valves. Herovici stains were preformed using Herovici's Collagen Stain Kit Procedure (American MasterTech, LODI, CA, Cat#KTHERPT). For immunohistochemistry (IHC): Antigen retrieval was performed for 1 minute using antigen unmasking solution (Vector Laboratories, Burlingame, CA, USA, Cat#H-3300) by pressure cooker (Cuisinart, Stamford, CT, USA). The following are the antibodies and their dilutions; Acetylated Tubulin (Sigma, Cat#T6793, 1:500), Gamma Tubulin (Abcam, Cambridge, MA, USA, Cat#ab11317, 1:1000), Versican (gift from Stan Hoffman, Medical University of South Carolina, 1: 250), Collagen (gift from Stan Hoffman, Medical University of South Carolina, 1: 250), MF20 (DSHB, Iowa City, IA, USA, Concentrate, I:50), Ki67 (Abcam, Cat#ab16667, 1:250), Phospho-histone H3 (EMD Millipore, Darmstadt Germany, Cat#06-570, 1:250), Smoothened (LSBio, Seattle WA, Cat#LS-A2666, 1:250), Gli3 (Origene, Rockville MD, Cat#TA337186, 1:250). Primary antibody was detected using fluorescent secondary antibody, Goat anti-Mouse IgG Alexa fluor 488 (Cat#A-11029, 1:100), Goat anti-Rabbit Alexa fluor 488 (Cat#A-11034, 1:100) anti-Mouse Alexa fluor 568 (Cat#A-11004, 1:100), anti-Rabbit Alexa fluor 568 (Cat#A-11036, 1:100) Cy5 goat anti-Mouse (Cat#A-10524, 1:100) and Cy5 goat anti-Rabbit (Cat#A-10523, 1:100) (Life Technologies, Rockville, MD, US). Nuclei were counterstained with Hoechst (Life Technologies, Cat #H3569, 1:10,000) for 10 minutes and slides were cover slipped with Slow Fade mounting medium (Life Technologies, Cat#S36937). Fluorescence imaging was preformed using Zeiss Axioimager M2 and Leica TCS SP5 AOBS Confocal Microscope System (Leica Microsystems, Inc., 410 Eagleview Boulevard, Suite 107, Exton, PA 19341). Z-stacks were set by finding the highest and lowest depth with visible fluorescence and using the system optimized setting to determine steps. Z-stacks were then compiled to form maximum projection images.

3D reconstruction

3D reconstructions of H and E images were preformed to generate volumetric measurements of postnatal day 0 right, left, and non-coronary leaflets, similar to previous reports (Durst et al., 2015). Briefly, 5 μm sections throughout the entirety h of the aortic cusps were H and E stained and imaged using the Olympus BX40 bright field microscope. Images were then aligned using ImageJ FIJI and imported into Imaris 8.0. Manual reconstruction was performed by tracing each individual cusp on every section and combining all traces to create a 3D structure. A total of 28 knockout and 15 wildtype animals were analyzed for BAV. Additionally, 3D reconstructions of immunohistochemistry were performed by importing confocal Z-stack images of 15um sections into Imaris and creating surface renderings based on intensity of the stains.

Quantifications

Cilia length measurements were performed using Z-stack images of right coronary cusps stained with acetylated alpha tubulin, gamma tubulin and counterstained with Hoechst. Z-stack images were then imported into Imaris software and measurements were taken from the base to the tip of the axoneme. All cilia in the field of view were measured, n=3 per developmental time point. Measurements were then ranked and grouped; zero microns represents absence of cilia. Quantification of cilia length in versican and collagen regions was performed on left coronary leaflets in the same way, n=3. Average cilia length was then calculated and Student's t-test was performed ($p<0.001$).

Cell density quantifications were measured by counting all nuclei in a specified area, 25.4mm^2 for post-natal measurement and 22 mm^2 for adult measurements. Post-natal measurements were taken at the base and tip of the right coronary leaflets, n=3. Adult measurements were taken at the tip of right coronary leaflets, n=3. Measurements were compared to wild-type data to generate fold change and statistical significance was calculated using a Student's *t*-test ($p<0.001$). Determination of collagen and versican expressing area was calculated by quantifying the area covered by each of these markers compared to the overall surface area of the cusp. This was performed on 3 sections from 3 independent control and conditional knockout (*NfatC1*$^{Cre(+)}$;*Ift88*$^{f/f}$) animals. Measurements were compared to wild-type data to generate actual percentage of valve area covered and statistical significance was calculated using a Student's *t*-test ($p<0.005$).

Quantification of Collagen was preformed using Herovici stained right coronary leaflets. Surface area of red staining was measured in Image J and percentages were calculated based on total leaflet surface area. n=3, with three areas per animal measured.

Acknowledgments

This work was supported in part by grants from the VA (Merit Award I01 BX000820 to J.H.L), NIH (P30DK074038 to J.H.L., R01HL131546 to R.A.N., P20GM103444 to R.A.N., R01HL127692 to R.A.N, R01HL114823 to S.J.B., RO1HL122906 to A.W, T32HL007260 to D.F and K.A.T, T35 DK 007431 to N.P.), and American Heart Association (GIA25080052 to R.A.N, and 16PRE30970048 to K.A.T). R.A.N. performed work in a facility constructed with support from a National Institutes of Health (NIH) grant (C06 RR018823)

Grant sponsor and number:

This work was supported in part by grants from the VA (Merit Award I01 BX000820 to J.H.L), NIH (P30DK074038 to J.H.L., R01HL131546 to R.A.N., P20GM103444 to R.A.N., R01HL127692 to R.A.N, R01HL114823 to S.J.B., RO1HL122906 to A.W, T32HL007260 to D.F and K.A.T, T35 DK 007431 to N.P.), and American Heart Association (GIA25080052 to R.A.N, and 16PRE30970048 to K.A.T). R.A.N. performed work in a facility constructed with support from a National Institutes of Health (NIH) grant (C06 RR018823)

References Cited

Baujat G, Le Merrer M. Ellis-van Creveld syndrome. Orphanet J Rare Dis. 2007; 2:27. [PubMed: 17547743]

Bitgood MJ, McMahon AP. Hedgehog and Bmp genes are coexpressed at many diverse sites of cell-cell interaction in the mouse embryo. Dev Biol. 1995; 172:126–138. [PubMed: 7589793]

Bonachea EM, Chang SW, Zender G, LaHaye S, Fitzgerald-Butt S, McBride KL, Garg V. Rare GATA5 sequence variants identified in individuals with bicuspid aortic valve. Pediatr Res. 2014a; 76:211–216. [PubMed: 24796370]

Bonachea EM, Zender G, White P, Corsmeier D, Newsom D, Fitzgerald-Butt S, Garg V, McBride KL. Use of a targeted, combinatorial next-generation sequencing approach for the study of bicuspid aortic valve. BMC Med Genomics. 2014b; 7:56. [PubMed: 25260786]

Broekhuis JR, Leong WY, Jansen G. Regulation of cilium length and intraflagellar transport. Int Rev Cell Mol Biol. 2013; 303:101–138. [PubMed: 23445809]

Broekhuis JR, Verhey KJ, Jansen G. Regulation of cilium length and intraflagellar transport by the RCK-kinases ICK and MOK in renal epithelial cells. PLoS One. 2014; 9:e108470. [PubMed: 25243405]

Cherian MP, Al-Sanna'a NA. Clinical spectrum of Bardet-Biedl syndrome among four Saudi Arabian families. Clin Dysmorphol. 2009; 18:188–194. [PubMed: 19707123]

Christensen ST, Pedersen SF, Satir P, Veland IR, Schneider L. The primary cilium coordinates signaling pathways in cell cycle control and migration during development and tissue repair. Curr Top Dev Biol. 2008; 85:261–301. [PubMed: 19147009]

Clement CA, Ajbro KD, Koefoed K, Vestergaard ML, Veland IR, Henriques de Jesus MP, Pedersen LB, Benmerah A, Andersen CY, Larsen LA, Christensen ST. TGF-beta signaling is associated with endocytosis at the pocket region of the primary cilium. Cell Rep. 2013a; 3:1806–1814. [PubMed: 23746451]

Clement DL, Mally S, Stock C, Lethan M, Satir P, Schwab A, Pedersen SF, Christensen ST. PDGFRalpha signaling in the primary cilium regulates NHE1-dependent fibroblast migration via coordinated differential activity of MEK1/2-ERK1/2-p90RSK and AKT signaling pathways. J Cell Sci. 2013b; 126:953–965. [PubMed: 23264740]

Daoud G, Kempf H, Kumar D, Kozhemyakina E, Holowacz T, Kim DW, Ionescu A, Lassar AB. BMP-mediated induction of GATA4/5/6 blocks somitic responsiveness to SHH. Development. 2014; 141:3978–3987. [PubMed: 25294942]

de Vlaming A, Sauls K, Hajdu Z, Visconti RP, Mehesz AN, Levine RA, Slaugenhaupt SA, Hagege A, Chester AH, Markwald RR, Norris RA. Atrioventricular valve development: new perspectives on an old theme. Differentiation. 2012; 84:103–116. [PubMed: 22579502]

Delling M, DeCaen PG, Doerner JF, Febvay S, Clapham DE. Primary cilia are specialized calcium signalling organelles. Nature. 2013; 504:311–314. [PubMed: 24336288]

Deveault C, Billingsley G, Duncan JL, Bin J, Theal R, Vincent A, Fieggen KJ, Gerth C, Noordeh N, Traboulsi EI, Fishman GA, Chitayat D, Knueppel T, Millan JM, Munier FL, Kennedy D, Jacobson SG, Innes AM, Mitchell GA, Boycott K, Heon E. BBS genotype-phenotype assessment of a multiethnic patient cohort calls for a revision of the disease definition. Hum Mutat. 2011; 32:610–619. [PubMed: 21344540]

Dina C, Bouatia-Naji N, Tucker N, Delling FN, Toomer K, Durst R, Perrocheau M, Fernandez-Friera L, Solis J, Le Tourneau T, Chen MH, Probst V, Bosse Y, Pibarot P, Zelenika D, Lathrop M, Hercberg S, Roussel R, Benjamin EJ, Bonnet F, Lo SH, Dolmatova E, Simonet F, Lecointe S, Kyndt F, Redon R, Le Marec H, Froguel P, Ellinor PT, Vasan RS, Bruneval P, Markwald RR, Norris RA, Milan DJ, Slaugenhaupt SA, Levine RA, Schott JJ, Hagege AA, Mvp F, Jeunemaitre X, Leducq Transatlantic MN. investigators P. Genetic association analyses highlight biological pathways underlying mitral valve prolapse. Nat Genet. 2015

Dupuis LE, Osinska H, Weinstein MB, Hinton RB, Kern CB. Insufficient versican cleavage and Smad2 phosphorylation results in bicuspid aortic and pulmonary valves. J Mol Cell Cardiol. 2013; 60:50–59. [PubMed: 23531444]

Durst R, Sauls K, Peal DS, deVlaming A, Toomer K, Leyne M, Salani M, Talkowski ME, Brand H, Perrocheau M, Simpson C, Jett C, Stone MR, Charles F, Chiang C, Lynch SN, Bouatia-Naji N, Delling FN, Freed LA, Tribouilloy C, Le Tourneau T, LeMarec H, Fernandez-Friera L, Solis J, Trujillano D, Ossowski S, Estivill X, Dina C, Bruneval P, Chester A, Schott JJ, Irvine KD, Mao Y, Wessels A, Motiwala T, Puceat M, Tsukasaki Y, Menick DR, Kasiganesan H, Nie X, Broome AM, Williams K, Johnson A, Markwald RR, Jeunemaitre X, Hagege A, Levine RA, Milan DJ, Norris RA, Slaugenhaupt SA. Mutations in DCHS1 cause mitral valve prolapse. Nature. 2015

Echelard Y, Epstein DJ, St-Jacques B, Shen L, Mohler J, McMahon JA, McMahon AP. Sonic hedgehog, a member of a family of putative signaling molecules, is implicated in the regulation of CNS polarity. Cell. 1993; 75:1417–1430. [PubMed: 7916661]

Egorova AD, Khedoe PP, Goumans MJ, Yoder BK, Nauli SM, ten Dijke P, Poelmann RE, Hierck BP. Lack of primary cilia primes shear-induced endothelial-to-mesenchymal transition. Circ Res. 2011; 108:1093–1101. [PubMed: 21393577]

Elbedour K, Zucker N, Zalzstein E, Barki Y, Carmi R. Cardiac abnormalities in the Bardet-Biedl syndrome: echocardiographic studies of 22 patients. Am J Med Genet. 1994; 52:164–169. [PubMed: 7802002]

Friedland-Little JM, Hoffmann AD, Ocbina PJ, Peterson MA, Bosman JD, Chen Y, Cheng SY, Anderson KV, Moskowitz IP. A novel murine allele of Intraflagellar Transport Protein 172 causes a syndrome including VACTERL-like features with hydrocephalus. Hum Mol Genet. 2011; 20:3725–3737. [PubMed: 21653639]

Garg V, Muth AN, Ransom JF, Schluterman MK, Barnes R, King IN, Grossfeld PD, Srivastava D. Mutations in NOTCH1 cause aortic valve disease. Nature. 2005; 437:270–274. [PubMed: 16025100]

Grisanti L, Revenkova E, Gordon RE, Iomini C. Primary cilia maintain corneal epithelial homeostasis by regulation of the Notch signaling pathway. Development. 2016; 143:2160–2171. [PubMed: 27122169]

Haycraft CJ, Zhang Q, Song B, Jackson WS, Detloff PJ, Serra R, Yoder BK. Intraflagellar transport is essential for endochondral bone formation. Development. 2007; 134:307–316. [PubMed: 17166921]

Hinton RB Jr, Alfieri CM, Witt SA, Glascock BJ, Khoury PR, Benson DW, Yutzey KE. Mouse heart valve structure and function: echocardiographic and morphometric analyses from the fetus through the aged adult. Am J Physiol Heart Circ Physiol. 2008; 294:H2480–2488. [PubMed: 18390820]

Hinton RB Jr, Lincoln J, Deutsch GH, Osinska H, Manning PB, Benson DW, Yutzey KE. Extracellular matrix remodeling and organization in developing and diseased aortic valves. Circ Res. 2006; 98:1431–1438. [PubMed: 16645142]

Hoffmann AD, Peterson MA, Friedland-Little JM, Anderson SA, Moskowitz IP. sonic hedgehog is required in pulmonary endoderm for atrial septation. Development. 2009; 136:1761–1770. [PubMed: 19369393]

Hoffmann AD, Yang XH, Burnicka-Turek O, Bosman JD, Ren X, Steimle JD, Vokes SA, McMahon AP, Kalinichenko VV, Moskowitz IP. Foxf genes integrate tbx5 and hedgehog pathways in the second heart field for cardiac septation. PLoS Genet. 2014; 10:e1004604. [PubMed: 25356765]

Huang H, Cotton JL, Wang Y, Rajurkar M, Zhu LJ, Lewis BC, Mao J. Specific requirement of Gli transcription factors in Hedgehog-mediated intestinal development. J Biol Chem. 2013; 288:17589–17596. [PubMed: 23645682]

Ishikawa H, Marshall WF. Ciliogenesis: building the cell's antenna. Nat Rev Mol Cell Biol. 2011; 12:222–234. [PubMed: 21427764]

Jin X, Muntean BS, Aal-Aaboda MS, Duan Q, Zhou J, Nauli SM. L-type calcium channel modulates cystic kidney phenotype. Biochim Biophys Acta. 2014; 1842:1518–1526. [PubMed: 24925129]

Karp N, Grosse-Wortmann L, Bowdin S. Severe aortic stenosis, bicuspid aortic valve and atrial septal defect in a child with Joubert Syndrome and Related Disorders (JSRD) - a case report and review of congenital heart defects reported in the human ciliopathies. Eur J Med Genet. 2012; 55:605–610. [PubMed: 22910529]

Levame M, Meyer F. Herovici's picropolychromium. Application to the identification of type I and III collagens. Pathol Biol (Paris). 1987; 35:1183–1188. [PubMed: 2446240]

Levin LS, Perrin JC, Ose L, Dorst JP, Miller JD, McKusick VA. A heritable syndrome of craniosynostosis, short thin hair, dental abnormalities, and short limbs: cranioectodermal dysplasia. J Pediatr. 1977; 90:55–61. [PubMed: 830894]

Li JB, Gerdes JM, Haycraft CJ, Fan Y, Teslovich TM, May-Simera H, Li H, Blacque OE, Li L, Leitch CC, Lewis RA, Green JS, Parfrey PS, Leroux MR, Davidson WS, Beales PL, Guay-Woodford LM, Yoder BK, Stormo GD, Katsanis N, Dutcher SK. Comparative genomics identifies a flagellar and basal body proteome that includes the BBS5 human disease gene. Cell. 2004; 117:541–552. [PubMed: 15137946]

Li L, Grausam KB, Wang J, Lun MP, Ohli J, Lidov HG, Calicchio ML, Zeng E, Salisbury JL, Wechsler-Reya RJ, Lehtinen MK, Schuller U, Zhao H. Sonic Hedgehog promotes proliferation of

Notch-dependent monociliated choroid plexus tumour cells. Nat Cell Biol. 2016; 18:418–430. [PubMed: 26999738]

Li Y, Klena NT, Gabriel GC, Liu X, Kim AJ, Lemke K, Chen Y, Chatterjee B, Devine W, Damerla RR, Chang C, Yagi H, San Agustin JT, Thahir M, Anderton S, Lawhead C, Vescovi A, Pratt H, Morgan J, Haynes L, Smith CL, Eppig JT, Reinholdt L, Francis R, Leatherbury L, Ganapathiraju MK, Tobita K, Pazour GJ, Lo CW. Global genetic analysis in mice unveils central role for cilia in congenital heart disease. Nature. 2015; 521:520–524. [PubMed: 25807483]

Lienkamp S, Ganner A, Walz G. Inversin, Wnt signaling and primary cilia. Differentiation. 2012; 83:S49–55. [PubMed: 22206729]

Liu Y, Pathak N, Kramer-Zucker A, Drummond IA. Notch signaling controls the differentiation of transporting epithelia and multiciliated cells in the zebrafish pronephros. Development. 2007; 134:1111–1122. [PubMed: 17287248]

Lumiaho A, Ikaheimo R, Miettinen R, Niemitukia L, Laitinen T, Rantala A, Lampainen E, Laakso M, Hartikainen J. Mitral valve prolapse and mitral regurgitation are common in patients with polycystic kidney disease type 1. Am J Kidney Dis. 2001; 38:1208–1216. [PubMed: 11728952]

Mangos S, Lam PY, Zhao A, Liu Y, Mudumana S, Vasilyev A, Liu A, Drummond IA. The ADPKD genes pkd1a/b and pkd2 regulate extracellular matrix formation. Dis Model Mech. 2010; 3:354–365. [PubMed: 20335443]

Martin PS, Kloessel B, Norris RA, Lindsay M, Milan D, Body SC. Embryonic Development of the Bicuspid Aortic Valve. Journal of Cardiovascular Development and Disease. 2015; 2:248–272. [PubMed: 28529942]

Mathieu P, Bosse Y, Huggins GS, Corte AD, Pibarot P, Michelena HI, Limongelli G, Boulanger MC, Evangelista A, Bedard E, Citro R, Body SC, Nemer M, Schoen FJ. The pathology and pathobiology of bicuspid aortic valve: State of the art and novel research perspectives. J Pathol Clin Res. 2015; 1:195–206. [PubMed: 27499904]

Michelena HI, Khanna AD, Mahoney D, Margaryan E, Topilsky Y, Suri RM, Eidem B, Edwards WD, Sundt TM 3rd, Enriquez-Sarano M. Incidence of aortic complications in patients with bicuspid aortic valves. JAMA. 2011; 306:1104–1112. [PubMed: 21917581]

Nandadasa S, Nelson CM, Apte SS. ADAMTS9-Mediated Extracellular Matrix Dynamics Regulates Umbilical Cord Vascular Smooth Muscle Differentiation and Rotation. Cell Rep. 2015; 11:1519–1528. [PubMed: 26027930]

Niggemann B, Muller A, Nolte A, Schnoy N, Wahn U. Abnormal length of cilia--a cause of primary ciliary dyskinesia--a case report. Eur J Pediatr. 1992; 151:73–75. [PubMed: 1728552]

Pazour GJ, Dickert BL, Vucica Y, Seeley ES, Rosenbaum JL, Witman GB, Cole DG. Chlamydomonas IFT88 and its mouse homologue, polycystic kidney disease gene tg737, are required for assembly of cilia and flagella. J Cell Biol. 2000; 151:709–718. [PubMed: 11062270]

Rawlins JM, Lam WL, Karoo RO, Naylor IL, Sharpe DT. Quantifying collagen type in mature burn scars: a novel approach using histology and digital image analysis. J Burn Care Res. 2006; 27:60–65. [PubMed: 16566538]

Salonen R. The Meckel syndrome: clinicopathological findings in 67 patients. Am J Med Genet. 1984; 18:671–689. [PubMed: 6486167]

Samsa LA, Givens C, Tzima E, Stainier DY, Qian L, Liu J. Cardiac contraction activates endocardial Notch signaling to modulate chamber maturation in zebrafish. Development. 2015; 142:4080–4091. [PubMed: 26628092]

Sauls K, Tommer K, Johnson A, RAN. Hematopoietic Derived Cells Contribute to Disease in the Filamin-A Model of Myxomatous Valvular Dystrophy. Journal of Cardiovascular Development and Disease. 2015 In Review.

Schneider L, Clement CA, Teilmann SC, Pazour GJ, Hoffmann EK, Satir P, Christensen ST. PDGFRalphaalpha signaling is regulated through the primary cilium in fibroblasts. Curr Biol. 2005; 15:1861–1866. [PubMed: 16243034]

Seeger-Nukpezah T, Golemis EA. The extracellular matrix and ciliary signaling. Curr Opin Cell Biol. 2012; 24:652–661. [PubMed: 22819513]

Sun Z, Amsterdam A, Pazour GJ, Cole DG, Miller MS, Hopkins N. A genetic screen in zebrafish identifies cilia genes as a principal cause of cystic kidney. Development. 2004; 131:4085–4093. [PubMed: 15269167]

Thompson CL, Chapple JP, Knight MM. Primary cilia disassembly down-regulates mechanosensitive hedgehog signalling: a feedback mechanism controlling ADAMTS-5 expression in chondrocytes. Osteoarthritis Cartilage. 2014; 22:490–498. [PubMed: 24457103]

Tory K, Rousset-Rouviere C, Gubler MC, Moriniere V, Pawtowski A, Becker C, Guyot C, Gie S, Frishberg Y, Nivet H, Deschenes G, Cochat P, Gagnadoux MF, Saunier S, Antignac C, Salomon R. Mutations of NPHP2 and NPHP3 in infantile nephronophthisis. Kidney Int. 2009; 75:839–847. [PubMed: 19177160]

Tzemos N, Therrien J, Yip J, Thanassoulis G, Tremblay S, Jamorski MT, Webb GD, Siu SC. Outcomes in adults with bicuspid aortic valves. JAMA. 2008; 300:1317–1325. [PubMed: 18799444]

Veland IR, Awan A, Pedersen LB, Yoder BK, Christensen ST. Primary cilia and signaling pathways in mammalian development, health and disease. Nephron Physiol. 2009; 111:p39–53. [PubMed: 19276629]

Wu B, Zhang Z, Lui W, Chen X, Wang Y, Chamberlain AA, Moreno-Rodriguez RA, Markwald RR, O'Rourke BP, Sharp DJ, Zheng D, Lenz J, Baldwin HS, Chang CP, Zhou B. Endocardial cells form the coronary arteries by angiogenesis through myocardial-endocardial VEGF signaling. Cell. 2012; 151:1083–1096. [PubMed: 23178125]

Yuan S, Li J, Diener DR, Choma MA, Rosenbaum JL, Sun Z. Target-of-rapamycin complex 1 (Torc1) signaling modulates cilia size and function through protein synthesis regulation. Proc Natl Acad Sci U S A. 2012; 109:2021–2026. [PubMed: 22308353]

Zhou B, Cron RQ, Wu B, Genin A, Wang Z, Liu S, Robson P, Baldwin HS. Regulation of the murine Nfatc1 gene by NFATc2. J Biol Chem. 2002; 277:10704–10711. [PubMed: 11786533]

Bullet points

- Primary cilia are regulated in a spatial-temporal manner during aortic valve development.
- In vivo genetic analyses demonstrate that primary cilia function to restrain ECM production
- Loss of cilia cause a highly penetrant bicuspid aortic valve disease phenotype

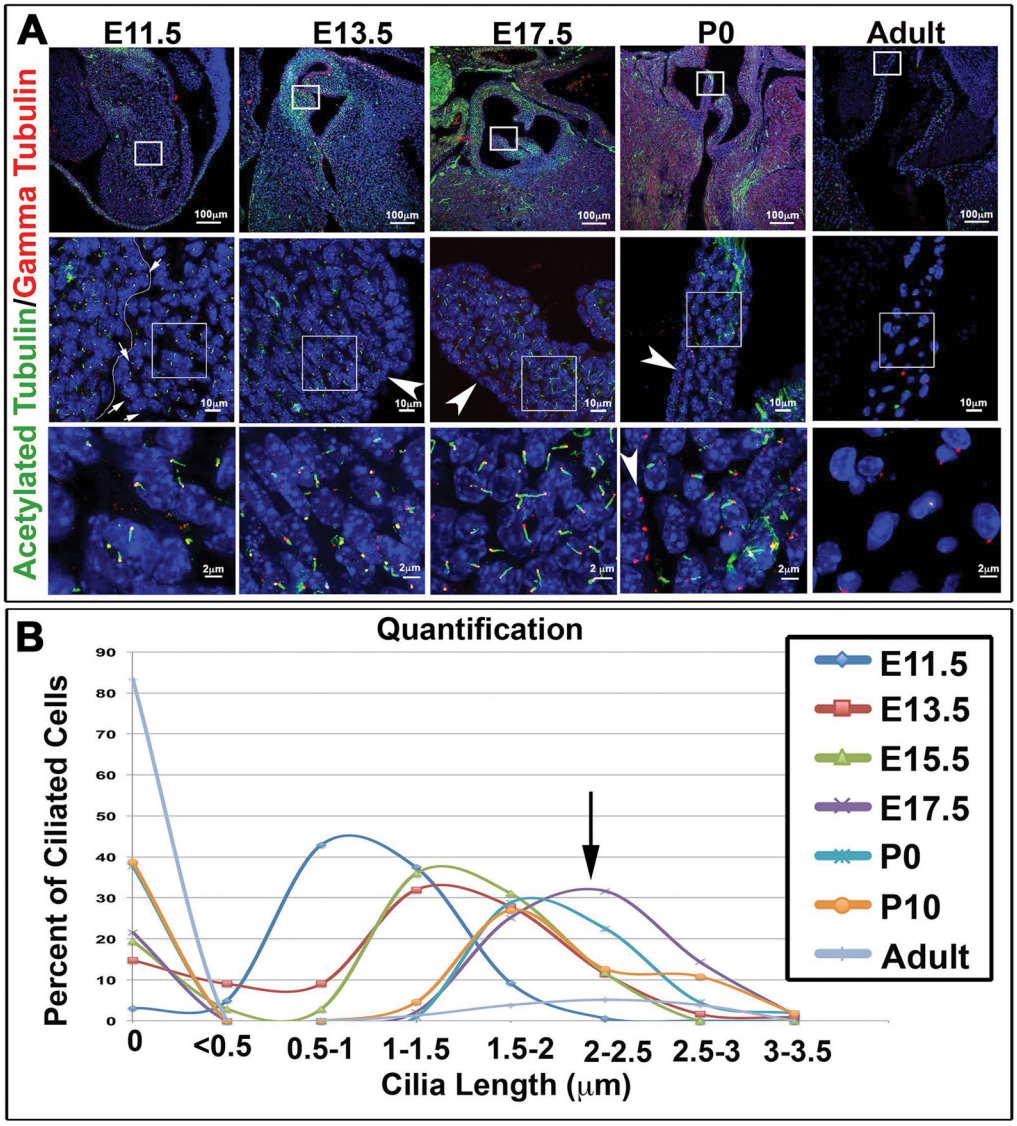

Figure 1. Expression of primary cilia during aortic valve development

(A) IHC for the ciliary axoneme (green), basal body (red), and nuclei (blue) show expression of cilia throughout valve development. Cilia appear shorter during early embryonic stages and longer right before and after birth. Arrows at E11.5 depict very short axonemes on endothelial cells (line depicting the edge of the endocardium is denoted) whereas arrowheads at the over timepoints depict lack of primary cilia on the valve endocardium at later timepoints (**B**) Quantification of cilia length showing increased expression of cilia during embryonic development, peaking at the E17.5 timepoint (purple line and arrow) and decreased expression during postnatal development and adult life.

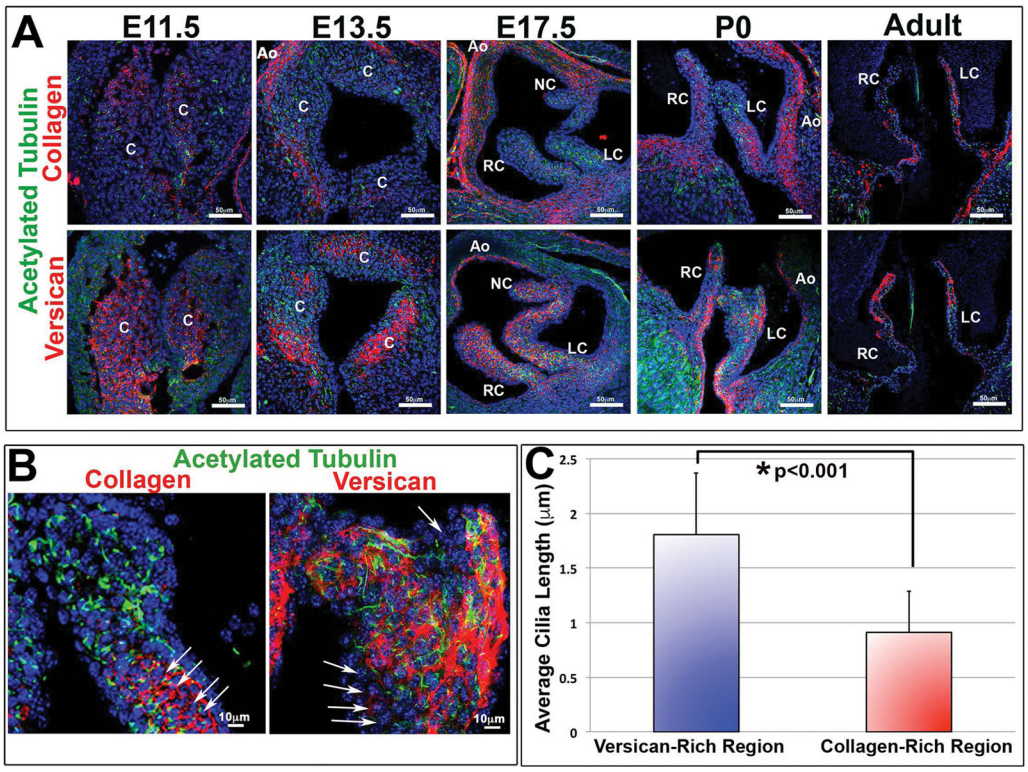

Figure 2. Correlation of primary cilia with versican expressing microenvironments

(**A**) IHC for the ciliary axoneme (green), collagen (red, top) versican (red, bottom), and nuclei (blue) show spatial/temporal expression of cilia throughout development. Cilia are predominantly expressed in proteoglycan-rich zones and scant in regions of high collagen expression. C= conal cushions, RC= right-coronary, LC= left-coronary, NC= non-coronary, Ao= aorta. (**B**) High magnification images of axonemes (green) and collagen/versican (red). Arrows depict collagen rich regions expressing shortened cilia. (**C**) Quantification of cilia length in both versican and collagen rich regions shows decreased average cilia length in collagen rich regions when compared with versican rich regions, $p<0.001$ Students t-test.

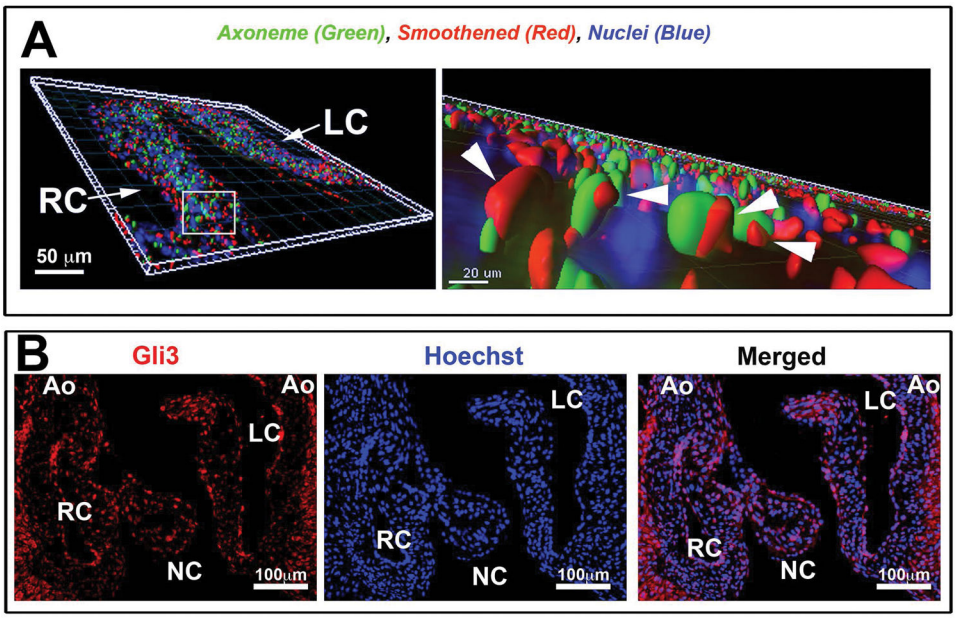

Figure 3. Active Hedgehog signaling in aortic valve interstitial cells in vivo

(**A**) Three-dimensional reconstruction of IHC stain at postnatal day 0, shows smoothened (red), acetylated tubulin—cilia axoneme (green), and Hoechst--nuclei (blue). High magnification (right) shows smoothened (arrowhead pointing to smoothened staining) on the axoneme of the cilia indicative of active hedgehog signaling. (**B**) IHC of P0 aortic cusps showing Gli3 expression.

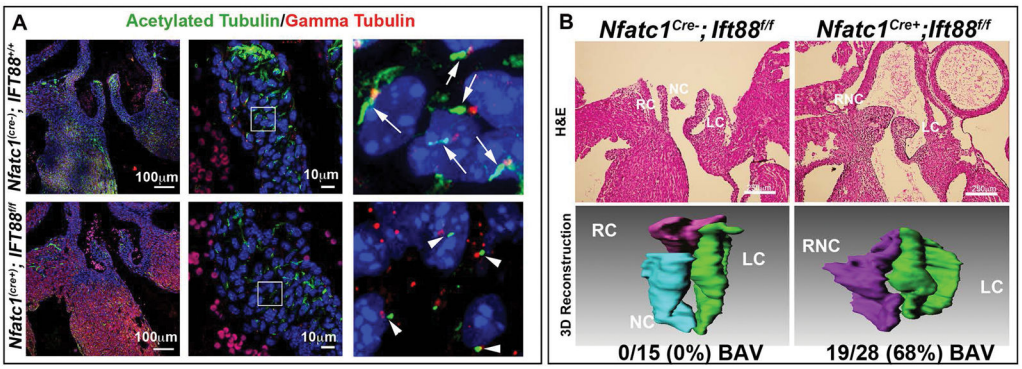

Figure 4. Developmental loss of axonemes causes BAV

(**A**) Control IHC experiments for the ciliary axoneme (green), basal body (red), and nuclei (blue) show normal cilia length on control aortic valves (top) vs. axoneme shortening in the *Ift88* conditional knockout (bottom). (**B**) H and E and 3D reconstruction of P0 wild type and conditional knockout valves. Wild-type valves show three distinct cusps while conditional knockout mouse aortic valves show bicuspid aortic valves. Penetrance of the phenotype is depicted below the 3D reconstruction images. RC=right coronary, LC= left coronary, NC= non-coronary, and RNC= right non-coronary.

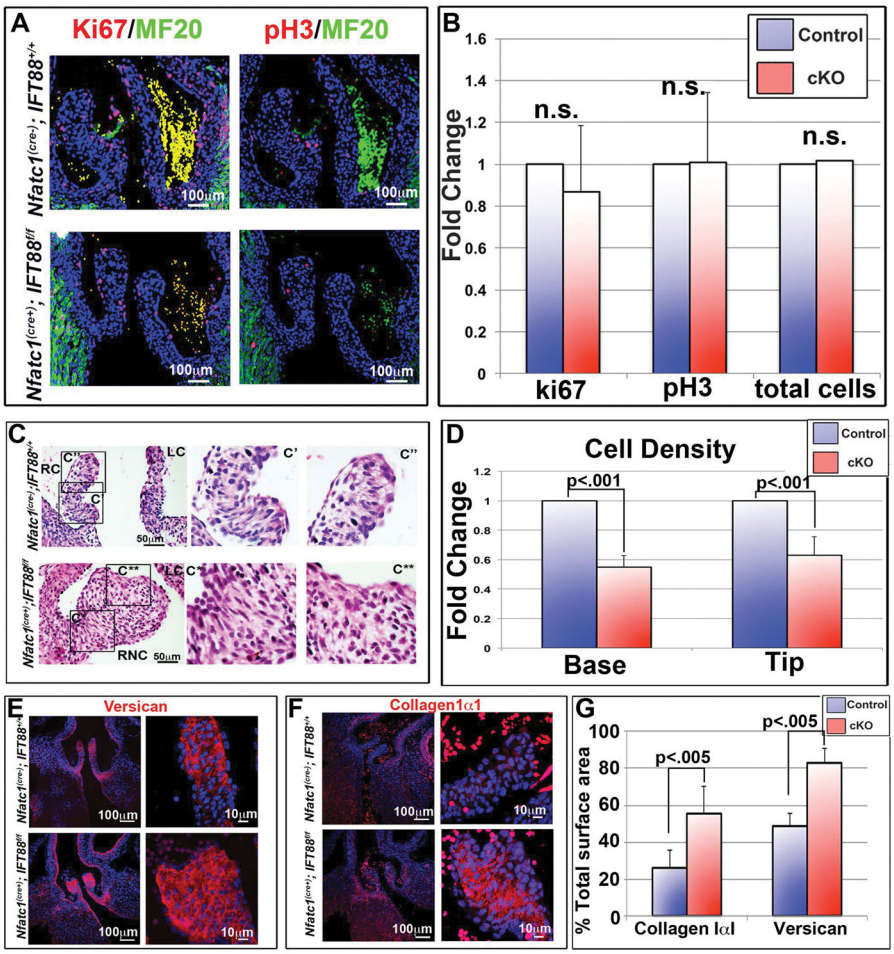

Figure 5. Cilia effects on proliferation and ECM production

(**A**) IHC of postnatal day 0 (P0) aortic valves, for proliferation markers Ki67 and phospho-histone H3, show no difference in proliferating or total cell number when conditional knockout aortic valves were compared to littermate controls, quantified in (**B**). (**C**) H and E staining's show increased matrix in the fused right-non-coronary leaflet of the conditional knockout. C′= wild-type right coronary, C″= wild-type right coronary tip, C*= conditional knockout right non-coronary base, C**= conditional knockout right coronary tip. RC= right coronary, LC= left coronary, RNC= right non-coronary. (**D**) Quantification of cell density shows a significant decrease in cell density in cilia deficient valves at both the base and tip of the right coronary leaflet, with p<.001. (**E and F**) IHC staining's of conditional knockout aortic cusps show increased expression of both collagen (**E**) and versican (**F**) in the cilia conditional knockout valves. (**G**) Quantification of total surface area occupied by collagen or versican immunostaining with p<.005. RC=right coronary, LC= left coronary, NC= non-coronary, and RNC= right non-coronary.

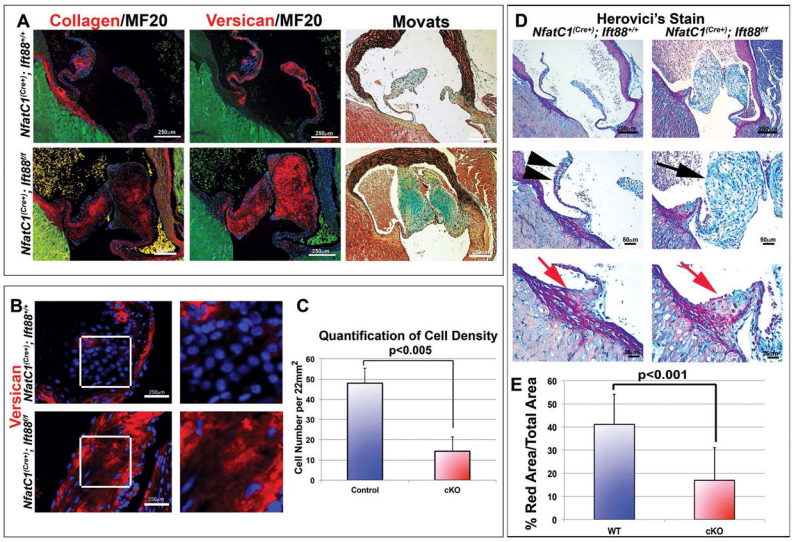

Figure 6. Loss of cilia results in myxomatous degeneration in adult aortic valves

(**A**) IHC and movats pentachrome stain of ECM proteins in adult mouse Nfatc1^{cre-};Ift88$^{+/+}$ and Nfatc1^{cre+};Ift88$^{f/f}$ aortic valves. Left and middle panels show IHC of collagen (red, left), versican (red, middle) MF20 (green), and nuclei (blue). Movats pentachrome stain (right) shows proteoglycans (blue), collagen (yellow), elastin (black), and fibrin or cardiac muscle (red). Increased expression of collagen and versican is observed in Ift88 conditional knockouts when compared to littermate controls in both IHC and movats stains. (**B**) IHC staining shows decreased cell density and increased versican in conditional knockout adult right coronary leaflets, quantified in (**C**) Student's T tests; $p<0.005$ n=3. Herovici's collagen stain shows decreased mature collagen (red) in conditional knockout cusps, quantified in (**D**) with $p<0.001$.